J Biomol NMR (2007) 39:315–322
DOI 10.1007/s10858-007-9202-6

ARTICLE

Effect of micelle interface on the binding of anticoccidial PW2 peptide

Luzineide W. Tinoco · Francisco Gomes-Neto · Ana Paula Valente · Fabio C. L. Almeida

Received: 29 May 2007 / Accepted: 18 September 2007 / Published online: 10 October 2007

Abstract PW2 is an anticoccidial peptide active against *Eimeria acervulina* and *Eimeria tenella*. We determined the structure of PW2 in dodecylphosphocholine micelles. The structure showed two distinct regions: an amphipathic N-terminal 3_{10} helix and an aromatic region containing WWR interface-binding motif. The aromatic region acted as a scaffold of the protein in the interface and shared the same structure in both DPC and SDS micelles. N-terminal helix interacted with DPC but not with SDS interface. Chemical shift change was slow when SDS was added to PW2 in DPC and fast when DPC was added to PW2 in SDS, indicating that interaction with DPC micelles was kinetically more stable than with SDS micelles. Also, DPC interface was able to accommodate PW2, but it maintained the conformational arrangement in the aromatic region observed for SDS micelles. This behavior, which is different from that observed for other antimicrobial peptides with WWR motif, may be associated with the absence of PW2 antibacterial activity and its selectivity for *Eimeria* parasites.

Keywords Avian coccidiosis · Antimicrobial peptide · *Eimeria* · Membrane · NMR · Structure

Deposits: PDB code 2JQ2 and BMRB accession number 15267.

Electronic supplementary material The online version of this article (doi:10.1007/s10858-007-9202-6) contains supplementary material, which is available to authorized users.

L. W. Tinoco
Nucleo de Pesquisas de Produtos Naturais, Universidade Federal do Rio de Janeiro, Rio de Janeiro, RJ 21941-590, Brazil

F. Gomes-Neto · A. P. Valente · F. C. L. Almeida (✉)
Centro Nacional de Ressonancia Magnetica Nuclear Jiri Jonas, Instituto de Bioquímica Médica, Programa de Biologia Estrutural, Universidade Federal do Rio de Janeiro, Rio de Janeiro, RJ 21941-590, Brazil
e-mail: falmeida@cnrmn.bioqmed.ufrj.br

Introduction

Avian coccidiosis is an intestinal disease caused by protozoan parasites of the genus *Eimeria*. It is one of the most important diseases in domestic poultry (Allen and Fetterer 2002). One approach to improving the control of avian coccidiosis is the development and use of anti-microbial peptides and derivatives (Martin et al. 1999).

Antimicrobial peptides share several features, such as structural diversity, cationic nature due to multiple Arg and/or Lys residues and amphipatic character (Zasloff 1992; Maloy and Kari 1995; Nicolas and Mor 1995). These properties allow binding of negatively charged surfaces of lipid membranes. Although it is well known that most natural antimicrobial peptides act by permeating membranes (Hancock et al. 1995; Lohner and Prenner 1999), the mechanism by which peptides kill is not fully understood. Anticoccidial peptide PW2 (HPLKQYWWRPSI) was selected from phage display libraries using living purified *Eimeria acervulina* sporozoites as targets. PW2 is active against sporozoites of avian *E. acervulina*, *E. tenella* and fungi, with poor or no activity against *Toxoplasma gondii* tachyzoites, *Trypanosoma cruzi*, *Crithidia fasciculata* epimastigotes, mammalian, avian cells and bacteria (DaSilva et al. 2002). The effectiveness against *Eimeria* sporozoites and the absence of adverse effects on host cells indicate that PW2 may be used as a model to develop new drugs for the control of avian

coccidiosis (DaSilva et al. 2002). PW2 disrupts the sporozoite pellicle through membrane permeabilization (DaSilva et al. 2002), similarly to other Trp-rich peptides with antimicrobial activity, such as indolicidin (Wu et al. 1999) and tritrpticin (Schibli et al. 1999).

Antimicrobial peptides have specificity for different types of plasmatic membrane (Lee 2001; Rilfors and Lindblom 2002; Vial et al. 2003), probably due to conformational transitions caused by the chemical nature of the interface. PW2 does not cause leakage in vesicles composed only of lipids containing phosphatidylcholine head groups, but it occurs in vesicles composed of a mixture of phosphatidylcholine and phosphatidylglycerol (DaSilva et al. 2002).

We solved the structure of PW2 by NMR in the presence of dodecylphosphocholine (DPC, present manuscript) and sodium dodecyl sulphate (SDS) micelles (Tinoco et al. 2002). PW2 was unstructured when free in solution, but it became structured in the presence of micelles. The small segment of PW2 containing the aromatic residues of the consensus sequence WWR (aromatic region) acquired the same structure both in SDS and DPC micelles. Based on chemical shift analyses and perturbation of the interface, it was found that the aromatic region is the peptide-interface anchor region. The structure of the aromatic region was interface-independent and thus intrinsic to the peptide. Also, N- and C-terminal regions acquired different structures in DPC and SDS, probably after the peptide was anchored to the interface.

Materials and methods

Sample preparation

The NMR sample of 3 mM PW2 in 300 mM DPC-d_{38} (Cambridge Isotope Laboratories—Andover, MA) was prepared in 20 mM aqueous sodium phosphate buffer (pH 5.0), 100 mM sodium chloride and 10% D_2O (99.9%—Isotec, Inc.).

NMR spectroscopy

NMR spectra were recorded at 25°C on a Bruker Avance DRX600 spectrometer operating at 600.04 MHz. TOCSY spectra (spin-lock time of 70 ms) were acquired using the MLEV-17 pulse sequence (Bax and Davis 1985). NOESY spectra were acquired using a 75 ms mixing time. Water suppression was achieved using the WATERGATE technique (Piotto et al. 1992; Sklenar et al. 1993). The spectra were collected with 4096 × 512 data points.

Addition of SDS to PW2 solubilized in DPC micelles

We added an aqueous solution of SDS to a sample containing 3 mM PW2 in 300 mM DPC. For each addition, final concentrations of 30 mM, 60 mM and 90 mM, respectively, were obtained (SDS-*d25* Cambridge Isotope Laboratories—Andover, MA). The addition of SDS resulted in dilution of PW2, DPC, buffer and NaCl. The final concentrations were as follows: for dilution 1–2.8 mM of PW2, 280 mM of DPC, 18.7 mM of phosphate buffer and 93.3 mM of NaCl; for dilution 2–2.6 mM of PW2, 262 mM of DPC, 17.5 mM of phosphate buffer and 87.3 mM of NaCl; for dilution 3–2.5 mM of PW2, 246 mM of DPC, 16.4 mM of phosphate buffer and 82.0 mM of NaCl. The DPC:SDS molar ratios were 9.3, 4.4 and 2.7 for dilutions 1, 2 and 3, respectively.

Addition of DPC to PW2 solubilized in SDS micelles

We added an aqueous solution of DPC-d_{38} to a sample containing 4 mM PW2 in 30 mM SDS, 20 mM of phosphate buffer, pH 5.0, 100 mM NaCl. The resulting DPC:SDS molar ratio was 10. After the addition of DPC, the final concentrations were 3.1 mM of PW2, 233 mM of DPC, 23.3 mM of SDS, 77 mM NaCl and 15.4 mM phosphate buffer, pH 5.0.

NMR data analysis and structure calculation

NMR data were processed with NMRPipe (Delaglio et al. 1995). All NMR spectra were analyzed using NMRVIEW, version 4.1.2 (Johnson and Blevins 1994). Distance constraints were calibrated using the NOE intensities of Tyr Hδ1–Hε1 of 2.4 Å. Structure calculations were performed using CNS-Solve version 1.1 (Brünger et al. 1998). Starting with the extended structure, 100 structures were generated using 10 ps (2,000 steps) of Cartesian simulated annealing at 1,000 K. We found that Cartesian simulated annealing explored well the conformational space and resulted in a better geometry. All the structures were analyzed with MOLMOL program (Koradi et al. 1996). Hydrogen bonds were analyzed by MOLMOL with a cutoff 2.4 Å for the distance between amidic hydrogen and carbonyl oxygen and 35° for the angle between the hydrogen bond and N–H bond.

Fluorescence measurements

Intrinsic fluorescence based on tryptophan emission spectra were analyzed in an ISS/K2 spectrofluorimeter (ISS, Champaign, IL) at 25°C. The samples were excited at

295 nm. PW2 samples (5 μM) were prepared in 20 mM sodium phosphate buffer, pH 5.0 containing 100 mM NaCl and were used with 10 mM DPC or SDS in the following DPC:SDS molar ratios 10, 5 and 3.3. For fluorescence quenching experiments, acrylamide concentration ranged from 10 to 100 mM. The Stern-Volmer coefficients (Ksv) for the quenching of the intrinsic tryptophan fluorescence by acrylamide for PW2 in the presence and absence of DPC and SDS were determined using the Stern-Volmer equation (Eftink and Ghiron 1976).

Results

We determined the solvent accessibility of the tryptophans of PW2 by intrinsic fluorescence quenching experiments. The Stern-Volmer coefficient (Ksv) expresses the quenching of the tryptophan fluorescence by acrylamide (Eftink and Ghiron 1976). High values of Ksv indicate higher accessibility of the tryptophan ring to acrylamide. Ksv value for PW2 in phosphate buffer was 12.8 M^{-1} and the maximum emission wavelength (λ_{max}) was 340 nm. Ksv decreased to 7.54 M^{-1} for PW2 in DPC, and 5.61 M^{-1} in SDS. It also decreased upon addition of SDS to DPC: 6.66 M^{-1} for [DPC]/[SDS] = 10, 6.16 M^{-1} for [DPC]/[SDS] = 5 and 5.87 M^{-1} for [DPC]/[SDS] = 3.3. The λ_{max} of emission decreased from 334 nm in DPC to 328 nm in SDS. The addition of SDS to DPC sample did not change the value of λ_{max}. This data indicated that Trp7 and Trp8 are less accessible to solvent in SDS than in DPC. The microenvironment in which PW2 is located in DPC is more polar and hydrated.

To identify the structural tendencies of PW2 in the presence of different interfaces we determined the NMR structure of PW2 in DPC micelles. The structure in SDS was already solved (Tinoco et al. 2002). DPC micelles form a zwitterionic interface and share a phosphocholine polar head group with natural lipids (Kallick et al. 1995; Baleja 2001).

The ^{1}H one-dimensional NMR spectra of PW2 as a function of DPC concentration (10 mM–300 mM) showed broad lines at low concentrations of DPC (10 mM–80 mM, data not shown), indicating that PW2 was in equilibrium between free and interface bound states. At higher concentration of DPC (above 100 mM, PW2:DPC molar ratio above 33.3), the binding equilibrium moved toward the bound state and produced sharp lines. Similar behavior was observed in SDS micelles (Tinoco et al. 2002).

Structure calculation

PW2 was fully assigned using the sequential strategy (Wüthrich 1986). The structures were convergent with all NOEs being compatible with the calculated family of structures, resulting in 100% of the torsion angles in the allowed region of the Ramachandran plot. Conformational averaging is more likely for peptides, especially in regions containing aromatics, resulting in violations of nonbonded contacts and also in the Ramachandran plot. However, none of these violations occurred in the present structures. The structure of PW2 in DPC displayed two distinct well-structured regions: (i) N-terminal amphipatic 3_{10} helix (Leu3-Lys4-Gln5-Tyr6) (Fig. 1a) and (ii) the aromatic region (Tyr6-Trp7-Trp8-Arg9) (Fig. 1b). Table 1 shows the structural statistics.

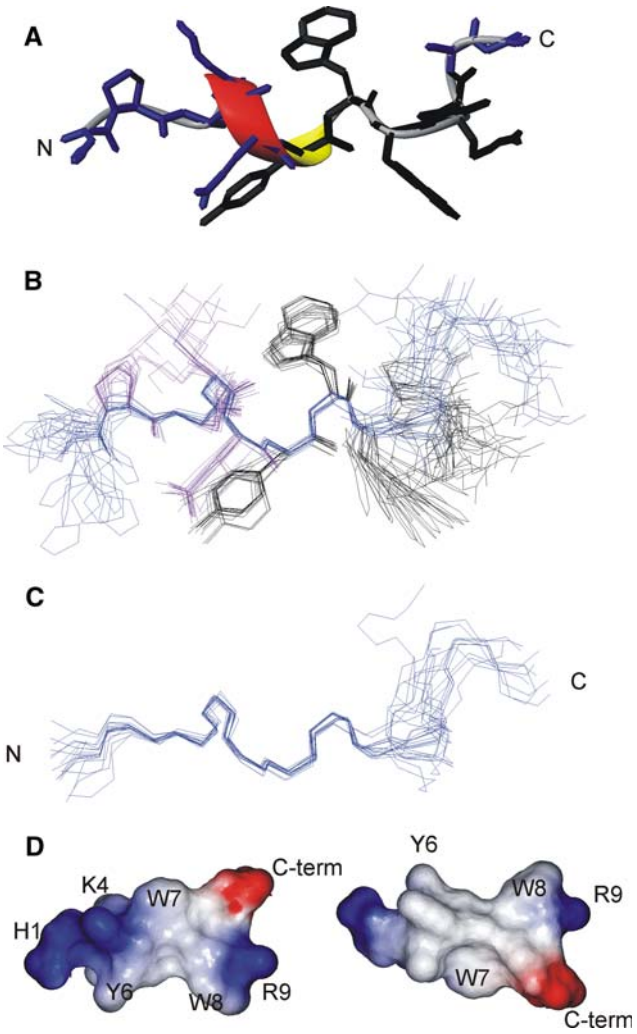

Fig. 1 Structures of PW2 in DPC micelles. (**a**) Ribbon representation of the average structure showing N-terminal helix, and the aromatic region. (**b**) 18 lowest energy structures showing all heavy atoms and (**c**) the backbone. N-terminal helix and the aromatic region: superposition of the backbone from residues 3 to 10 of the 18 lowest energy structures. (**d**) Two views (rotation 180° along the z axis) of surface potential of the lowest energy structure. Surface in red is negatively charged; in blue positively charged; white is used for neutral residues. The figure was obtained using the MOLMOL program (Koradi et al. 1996)

Table 1 Summary of structural statistics for PW2 in DPC micelles

Total no. of distance constraints	308
No. of intraresidue constraints	194
No. of sequential constraints	73
No. of medium-range constraints	41
No. of dihedral restraints ($^3J_{HNHA}$)	4
R.m.s. deviations from ideal geometry	
Bonds (Å)	0.0032 ± 0.00029
Angles (degrees)	0.549 ± 0.023
Improper (degrees)	0.259 ± 0.0216
Dihedral (degrees)	4.535 ± 0.782
NOE (Å)	0.0192 ± 0.0026
Energies (Kcal/mol)	
Overall	63.2 ± 5.27
Bond	3.58 ± 0.570
Angle	24.7 ± 2.25
Improper	1.53 ± 0.370
VDW (Lennard-Jones)	12.6 ± 4.68
NOE	9.78 ± 2.94
Pairwise rmsd (Å)	Total (18 structures)
Backbone (residues 1–12)	1.12
Heavy	1.76
Backbone (residues 3–10)	0.514
Heavy	1.23
Backbone (residues 2–7)	0.154
Heavy	1.01

The N-terminal amphipatic helix (Fig. 1a) displayed a NOE pattern typical of a 3_{10} helix (Wüthrich 1986), with intense NN(i, i + 1) NOEs, several αN(i, i + 2) and αN(i, i + 3) and also absence of αN(i, i + 4) NOEs. Several medium-range NOEs, typical of helices, stabilized this secondary structure (Table 2, supplementary Fig. 1). We measured in the calculated structures the presence of stable hydrogen bonds and noticed the presence of a hydrogen bond typical of a 3_{10} helix between Leu3 carbonyl and Tyr6 amide hydrogen (Wüthrich 1986). Please note we did not use hydrogen bonds constraints in the calculation.

The aromatic region contains the WWR interacting motif (Tinoco et al. 2002). The structure of this region depended mostly on NOEs connecting aromatic side chains, which represent 38% of all NOEs (118/308). They also were 63% (25/41) of all medium-range restraints. The aromatic region has a similar structure for PW2 in DPC and SDS, showing the same side-chain arrangement in both structures (Tinoco et al. 2002). The backbones are different, but the side chains orientation is exactly the same (Fig. 2a). This common structure suggests that this region acts a scaffold of the peptide, where the structure is independent of the environment.

Tyr6 and Trp7 side chains make NOE connections to all other parts of the peptide. Trp7 showed NOEs to both the

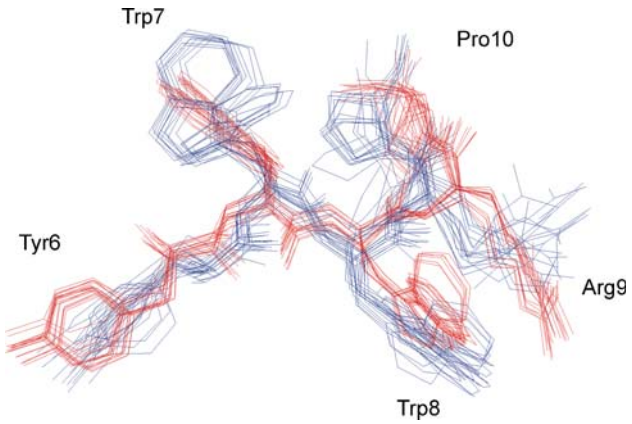

Fig. 2 Superposition of the structures of the aromatic region of PW2 in SDS (1M02, blue) and DPC (red). Note the similar folding of the aromatic region in both SDS and DPC

N-terminal helix (mainly with Lys4) and the C-terminal region (Pro10 and Ser11). Trp7 side chain is clustered between the Lys4 aliphatic chain and Pro10 (Fig. 1b), being stabilized by hydrophobic contacts. Tyr6, on the other hand, is common to both helical and aromatic regions. Several NOEs connecting Tyr6 to Leu3 stabilize the helix, and there are NOEs connecting Tyr6 within the aromatic region. Trp8 and Arg9 contribute to interface interaction, and there are several NOEs connecting Trp8 and Arg9 side chains, indicating a cation-π interaction contributing to the stabilization of the peptide structure. The structure in DPC was calculated using the topologies for both Pro2 and Pro10 in trans conformations. However, we observed two spin systems for Pro2, typical of cis-trans isomerization. For Pro10, on the other hand, we observed one spin system in the spectra, and NOEs indicating the presence of only trans conformation (H_α-ProH_δ (i, i + 1)).

As can be seen in Fig. 1d, PW2 structure is amphipathic. The aromatic side chains form a hydrophobic patch able to interact with the interface. Arg9, Lys4 and His1 make the peptide positive and possibly bind to the phosphate of DPC head group.

The difference between the observed chemical shifts and those in random coil reveals great changes, many of which are originated from ring current shifts. In fact, most of the hydrogens are shifted upfield, revealing that they are, on average, perpendicular to the plane of the aromatic ring, which is consistent with the calculated structure (see supplementary Table 1).

Comparison of the structure in DPC and SDS micelles

A comparison of the structures obtained in DPC and SDS revealed important conformational differences. Both the

similarities and differences are summarized in supplementary Table 2.

The aromatic region shows the same structure at both interfaces, while the N- and C-terminal region shows a different structure in SDS and DPC. The N-terminal region folds as a 3_{10} helix in DPC whereas in SDS it is bent toward Trp7 hiding Pro2 and Leu3 side chains from contact with water. In DPC, the interface is more complex in terms of chemical nature, enabling the folding into a helix. This helix is amphipatic, with Pro2 and Leu3 facing one side of the helix and Lys4, Gln5, the other side.

Binding properties of PW2 to DPC and SDS interface

The conformation of the aromatic region of PW2 was independent of the interface, whereas those of the N-terminal and C-terminal regions depended on the chemical nature of the interface. To map the residues at each region responsible for the binding to DPC interface, we probed the chemical shift changes of PW2 by modifying the DPC interface through the addition of SDS. Figure 3 displays the ^{1}H NMR spectra of the amidic and aromatic regions of PW2 in different DPC/SDS molar ratios and in pure DPC.

The use of SDS as perturbing agent enabled us to map residues making hydrogen bond contact with DPC head group. The chemical shift of most of the amide hydrogens did not vary significantly upon addition of SDS, except for the chemical shift of the indolic hydrogens of Trp7 and Trp8 and the amidic hydrogens of Leu3, Lys4 and Gln5 (Fig. 3a–e), which moved upfield. Such hydrogens were probably forming hydrogen bonds with the DPC head group and the addition of SDS would break them (Cordier and Grzesiek 2000). Changes in alpha hydrogens chemical shifts were very small after the addition of SDS.

It is remarkable that the kinetics of the change in chemical shifts was very slow. It took longer than 2 h to reach equilibrium when SDS was added to DPC. Figure 4a

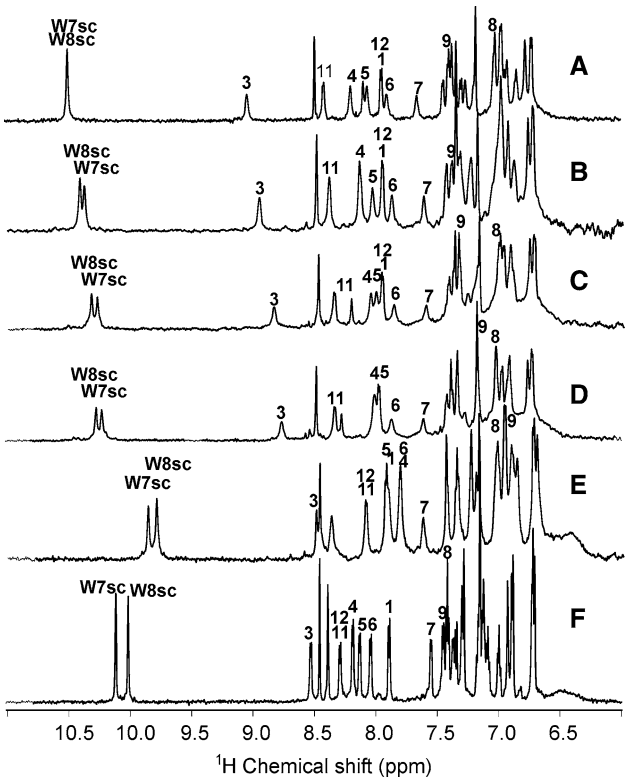

Fig. 3 Amidic and aromatic regions of ^{1}H one-dimensional NMR spectra of PW2 at 25°C. (**a**) In 300 mM of DPC; (**b**) in DPC:SDS molar ratio of 9.3; (**c**) in DPC:SDS molar ratio of 4.4; (**d**) in DPC:SDS molar ratio of 2.7; (**e**) in SDS 160 mM; (**f**) in 20 mM phosphate buffer at pH 5.0. See the material and methods section for the exact concentrations. The numbers 1–12 refer to the PW2 aminoacid number of amidic resonances and "sc" stands for side chain. All the spectra were obtained after equilibrium was reached

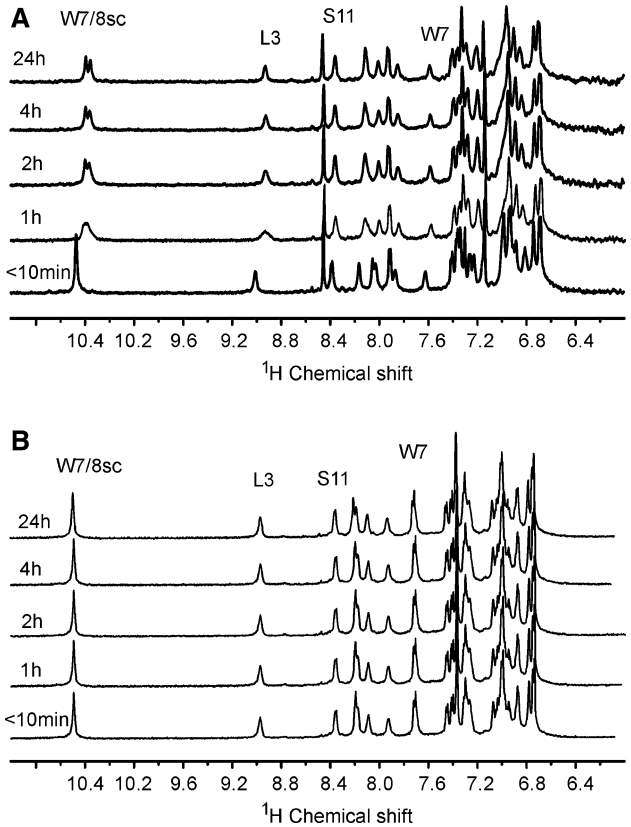

Fig. 4 ^{1}H one-dimensional NMR spectra of selected resonances (Leu-3 amidic and Trp-7/Trp-8 indolic hydrogens) as a function of time (**a**) after the addition of SDS to a solution of PW2 in 300 mM of DPC to a final DPC/SDS molar ratio of 9.3. Figure 3a shows the spectrum of PW2 in DPC before the addition of SDS. (**b**) After the addition of DPC to a solution of PW2 in 30 mM of SDS to a final DPC/SDS molar ratio of 10. The spectrum of PW2 in SDS, before the addition of DPC (not shown), is similar to that in Fig. 3e. Immediately after the addition of DPC, indolic resonances moved from ~9.8–10.43 ppm. Leu-3 resonances moved from ~8.5–8.92. Note that the endpoint reached in each of the experiments is not the same. See the material and methods section for the exact concentrations

shows the spectra of the amide and aromatic resonances (Leu3 amidic and Trp7/Trp8 indolic hydrogens) as a function of time after the addition of SDS to a final DPC:SDS molar ratio of 9.3. Note the line broadening after 1 h, indicating that conformational exchange occurred. The resulting spectra after addition of SDS to PW2 in DPC (Fig. 4a) and after addition of DPC to PW2 in SDS (Fig 4b) are slightly different. PW2 spectrum is dependent on sample preparation, such as salt concentration, pH, and detergent concentration. Also, note that endpoint is not the same in Fig. 4a and b. All the spectra in Fig. 3 were obtained after equilibrium was reached.

It is unusual for small peptides to change conformation in such a slow rate. However, PW2 conformation in DPC micelles was stabilized by the interaction with the interface. A kinetically stable interaction of PW2 with the DPC interface can explain this effect. PW2-DPC contacts should be broken to re-accommodate the newly formed SDS-DPC mixed interface. The highest chemical shift changes occurred for the interacting residues, which are the ones belonging to the amphipatic helix (Leu3, Lys4 and Gln5), the indolic hydrogens (Trp7 and 8) and the Arg9 amidic hydrogen (Figs. 3 and 4).

To compare the association of PW2 with the SDS and DPC interfaces, the reverse experiment was carried out. DPC was added to a solution of PW2 in SDS. In this case, all chemical shifts changes occurred immediately (Fig. 4b). The spectrum that resulted from this experiment (not shown) is very similar to the spectrum of PW2 in DPC (Fig. 3a and b). The kinetics of the conformational changes is more than two orders of magnitude faster for SDS, demanding thus more energy to change the conformation of PW2 when it is associated with DPC. This finding strongly suggests that interaction with DPC micelles is kinetically more stable than with SDS micelles.

Discussion

Several authors have reported major peptide conformation differences when structures in SDS and DPC micelles are compared (Yu et al. 2001; Hicks et al. 2003; Jing et al. 2003; Palian et al. 2003; Whitehead et al. 2004). Particularly, plasticity is of key importance in membrane specificity and biological function.

PW2 structure is also dependent on the environment. PW2 is flexible and unstructured when in aqueous solution. It gains structure upon binding to an interface. The difference in the structure of PW2 in both DPC and SDS (Tinoco et al. 2002) shows that plasticity makes it possible that the peptide can be accommodated at different interfaces. In this work, we attempted to determine structural rules for PW2 peptide, and we found that PW2 has at least two distinct regions: (i) a region whose structure is dependent on the interface, which would play a role in terms of specificity, and (ii) a membrane-anchoring region, whose structure is independent of the interface. These rules could generally be applied to membrane-acting peptides.

The structure of the aromatic region was similar for both SDS and DPC. Three aromatics residues compose this region (Tyr6, Trp7, Trp8). Their side chains can be superimposed (Fig. 2a) whereas the main chain is different in SDS and DPC, suggesting that the structure is stabilized by interactions of apolar aromatic side chains. It is worth noting that the steric effect is very important in stabilizing the conformation of the aromatic region. Intrinsic fluorescence measurements showed that, for both SDS and DPC, tryptophans are not accessible to the solvent, possibly being in contact with the interface in both micelles. Therefore, the aromatic region anchors the peptide to the micelles interface, similarly in SDS and DPC.

In addition, the other regions of PW2 are more plastic than the aromatic region. The structure of such regions is more dependent on the environment than on the peptide chain. The N-terminal region of PW2 presented different structures in SDS and DPC. It formed an amphipatic helix in DPC while in SDS it bent toward the Trp7 side chain. The interaction of PW2 with DPC interface allows the stabilization of a helix in the N-terminal region. This helix is not present in SDS, where the N-terminal chain is bent, keeping the apolar side chains of Pro2 and Leu3 far from water.

This behavior can be explained by the chemical nature of the interface, which favors the interaction with DPC. DPC have more sites available for the interaction with the peptide, such as phosphate, choline and aliphatic chains. It is also more hydrated. However, SDS interface displays only two interacting chemical groups: sulphate and the aliphatic chains. Note that fluorescence measurements showed that in SDS tryptophans are interacting in a more the hydrophobic environment. Probably, polar forces such as hydrogen bonds and electrostatic interaction are acting in stabilizing interaction of N-terminal helix with DPC interface. Intrinsic Trp fluorescence also corroborates this idea, showing that in DPC the tryptophans are in a more polar environment than in SDS. Neidigh and Andersen (2002) attributed these differences to an energetically favorable interaction of the tryptophan side chain with phosphocholine headgroups. The lower Ksv observed in SDS does not necessarily indicate that the interaction with SDS is stronger than with DPC. Rather it may show that DPC provides a more polar environment at the interface, enabling interactions such as those of hydrogen bonds, which are not present in SDS.

In SDS micelles, we have assigned the peptide in three situations. Free in solution, bound (high SDS

concentration) and at an intermediate situation (low SDS concentration). We mapped the lines that are broadened in the intermediate situation, which undergoes exchange between the free and bound PW2. We also mapped chemical shift differences in the three situations. Using this method, we found that the consensus sequence WWR is in direct contact with SDS interface (Tinoco et al. 2002).

For DPC, we did not observe an intense line broadening at low DPC concentration observed for PW2 in SDS. However, using SDS as a perturbing agent, we also obtained information on the residues in contact with the interface, as shown in Fig. 3. A similar strategy was used elsewhere (Whitehead et al. 2001). The addition of SDS to PW2 in DPC micelles led to upfield chemical shift changes in the indolic hydrogens of both Trp7 and Trp8 and amidic hydrogens such as Leu3 (Fig. 4). Upfield shifts of the amides if interpreted in terms of breakage of hydrogen bonds, occurred in the helix region, confirming the tendency to unfold the helix with increasing SDS concentration, and also between the peptide and the DPC interface, in the indolic amine of the tryptophans and interface.

We have observed chemical shift perturbation on slow kinetic when SDS was added to PW2 in DPC micelles, indicating the presence of a high-energy barrier (activation energy) for the conformational change of PW2 in mixed systems of SDS and DPC. This effect was only observed when SDS was added to PW2 in DPC. It did not occur when DPC was added to PW2 in SDS. In the latter case, changes in the spectra occurred on rapid timescale. The formation of mixed micelles is instantaneous. The peptide does not protect the entire DPC micelle from fast exchange with SDS monomer. Slow kinetics for PW2 in DPC was observed following resonances from the peptide, which indicated that the re-equilibration was not of the micelles but of the peptide conformation. This can be explained by a kinetically stable interaction of PW2 to DPC. The interaction most probably occurs with tightly bound DPC molecules within the micellar interface. The only spin system in the spectra that showed two separate sets of resonances was Pro2, due to *cis*-trans isomerization, which occurred in both DPC and SDS. This slow exchange between these two conformations could be the origin of the slow kinetic when SDS was added to PW2 in DPC. The N-terminal NH3+ and the positive side chain of His1 would attract SDS negative polar head. This could generate a kinetic trap, since the N-terminal region is better accommodated to DPC micelles. The role of Pro2 in this regard needs further investigation.

Structure-function studies of antimicrobial peptides indicate that a number of parameters modulate antibiotic activity, conformation, charge, overall hydrophobicity and amphipathicity (Blondelle and Houghten 1991; Shin et al. 2000; Yeaman and Yount 2003). Recent approaches have aimed to produce antimicrobial peptides that are more potent than native peptides towards the pathogen, without being toxic to mammalian cells. For example, the incorporation of D-amino acids into lytic peptides (Shai and Oren 1996), as well as central hinges induced by Pro residues (Subbalakshmi et al. 1996; Hong et al. 1999; Oh et al. 2000), or reduced amide bonds (Oh and Lee 2000) contributes to improving selective cytolytic activity. Furthermore, while Trp residues in several antimicrobial peptides are involved in hemolytic activity, Trp to Leu substitutions in indolicidin and melittin significantly reduce hemolytic activity but maintain antibacterial activity.

Whitehead and co-workers (2001) suggested that the binding of neuropeptides to both SDS and DPC micelles are controlled by hydrophobic interactions. We believe that for PW2 both ionic and hydrophobic interactions play important roles.

The antimicrobial hexapeptide Ac-RRWWRF-NH_2, displays a structure in DPC less well defined than that in SDS (Jing et al. 2003). Different from PW2, this peptide presents three positively charged residues, not presenting hydrophobic residues in the N-terminal portion. We consider that PW2 is more stabilized in DPC micelles because of the presence of hydrophobic residues in the N-terminal portion. Additionally, there is a smaller number of positively charged residues present in PW2.

Jing and co-workers (2003) suggest that the antimicrobial activity of Ac-RRWWRF-NH_2 is related to its greater capacity to interact with anionic SDS micelles, which would suggest a SDS a better model for bacterial cell membranes. The fact that PW2 accommodate better to DPC micelles when compared with SDS micelles could explain its inefficacy as an antibacterial. It remains to be determined whether this distinct behavior of PW2 for different micelle systems can be related to its selectivity for *Eimeria* parasites.

Acknowledgements This work was supported by CNPq, CNPq/PRONEX, FAPERJ and ICGEB-RELAB-OPS. We thank Monica Santos de Freitas for assistance with the fluorescence measurements and Catarina A. Miyamoto and Gisele C. Amorim for revising the manuscript.

References

Allen PC, Fetterer RH (2002) Recent advances in biology and immunobiology of *Eimeria* species and in diagnosis and control of infection with these coccidian parasites of poultry. Clin Microbiol Rev 15:58–65

Baleja JD (2001) Structure determination of membrane-associated proteins from nuclear magnetic resonance data. Anal Biochem 288:1–15

Bax A, Davis DG (1985) Mlev-17-based two-dimensional homonuclear magnetization transfer spectroscopy. J Magn Reson 65:355–360

Blondelle SE, Houghten RA (1991) Hemolytic and antimicrobial activities of the 24 individual omission analogs of melittin. Biochemistry 30:4671–4678

Brünger AT, Adams PD, Clore GM, DeLano WL, Gros P, Grosse-Kunstleve RW, Jiang JS, Kuszewski J, Nilges M, Pannu NS, Read RJ, Rice LM, Simonson T, Warren GL (1998) Crystallography & NMR system: A new software suite for macromolecular structure determination. Acta Crystallogr D Biol Crystallogr 54:D905–D921

Cordier F, Grzesiek S (2002) Temperature-dependence properties as studied by of protein hydrogen bond high-resolution NMR. J Mol Biol 715:739–752

Delaglio F, Grzesiek S, Zhu G, Vuister GW, Pfeifer J, Bax A (1995) NMRPIPE—a multidimensional spectral processing system based on unix pipes. J Biomol NMR 6:277–293

DaSilva A, Kawazoe U, Freitas FFT, Gatti MSV, Dolder H, Schumacher RI, Juliano MA, DaSilva MJ, Leite A (2002) Avian anticoccidial activity of a novel membrane-interactive peptide selected from phage display libraries. Mol Biochem Parasitol 120:53–60

Eftink MR, Ghiron CA (1976) Exposure of tryptophanyl residues in proteins—quantitative-determination by fluorescence quenching studies. Biochemistry 15:672–680

Hancock REW, Falla T, Brown M (1995) Cationic bactericidal peptides. Adv Microb Physiol 37:135–175

Hicks RP, Mones E, Kim H, Koser BW, Nichols DA, Bhattacharjee AK (2003) Comparison of the conformation and electrostatic surface properties of magainin peptides bound to sodium dodecyl sulfate and dodecylphosphocholine micelles. Biopolymers 68:459–470

Hong J, Oren Z, Shai Y (1999) Structure and organization of hemolytic and nonhemolytic diastereomers of antimicrobial peptides in membranes. Biochemistry 38:16963–16973

Jing W, Hunter HN, Hagel J, Vogel HJ (2003) The structure of the antimicrobial peptide Ac-RRWWRF-NH2 bound to micelles and its interactions with phospholipid bilayers. J Pept Res 61: 219–229

Johnson BA, Blevins RA (1994) NMRVIEW—a computer-program for the visualization and analysis of NMR data. J Biomol NMR 4:603–614

Kallick DA, Tessmer MR, Watts CR, Li CY (1995) The use of dodecylphosphocholine micelles in solution NMR. J Magn Reson 109:60–65

Koradi R, Billeter M, Wüthrich K (1996) MOLMOL: a program for display and analysis of macromolecular structures. J Mol Graph 14:51–55

Lee A (2001) Membrane structure. Curr Biol 20:R811–R814

Lohner K, Prenner EJ (1999) Differential scanning calorimetry and X-ray diffraction studies of the specificity of the interaction of antimicrobial peptides with membrane-mimetic systems. Biochim Biophys Acta 1462:141–156

Maloy WL, Kari UP (1995) Structure-activity studies on magainins and other host-defense peptides. Biopolymers 37:105–122

Martin A, Danforth HD, Jaynes JM (1999) Evaluation of the effect of peptidyl membrane-interactive molecules on avian coccidian. Parasitol Res 85:331–336

Neidigh JW, Andersen NH (2002) Peptide conformational changes induced by tryptophan-phosphocholine interactions in a micelle. Biopolymers 65:354–361

Nicolas P, Mor A (1995) Peptides as weapons against microorganisms in the chemical defense system of vertebrates. Annu Rev Microbiol 49:277–304

Oh JE, Lee KH (2000) Characterization of the unique function of a reduced amide bond in a cytolytic peptide that acts on phospholipid membranes. Biochem J 352:659–666

Oh D, Shin SY, Lee S, Kang JH, Kim SD, Ryu PD, Hahm KS, Kim Y (2000) Role of the hinge region and the tryptophan residue in the synthetic antimicrobial peptides, cecropin A(1–8)-magainin 2(1–12) and its analogues, on their antibiotic activities and structures. Biochemistry 39:11855–11864

Palian MM, Boguslavsky VI, O'Brien DF, Polt R (2003) Glycopeptide-membrane interactions: glycosyl enkephalin analogues adopt turn conformations by NMR and CD in amphipathic media. J Am Chem Soc 125:5823–5831

Piotto M, Saudek V, Sklenar V (1992) Gradient-tailored excitation for single-quantum nmr-spectroscopy of aqueous-solutions. J Biomol NMR 2:661–666

Rilfors L, Lindblom G (2002) Regulation of lipid composition in biological membranes—biophysical studies of lipids and lipid synthesizing enzymes. Colloid Surf B 26:112–124

Schibli DJ, Hwang PM, Vogel HJ (1999) Structure of the antimicrobial peptide tritrpticin bound to micelles: a distinct membrane-bound peptide fold. Biochemistry 38:16749–16755

Shai Y, Oren Z (1996) Diastereomers of cytolysins, a novel class of potent antibacterial peptides. J Biol Chem 271:7305–7308

Shin SY, Kang JH, Jang SY, Kim Y, Kim KL, Hahm KS (2000) Effects of the hinge region of cecropin A(1–8)-magainin 2(1–12), a synthetic antimicrobial peptide, on liposomes, bacterial and tumor cells. Biochim Biophys Acta 1463:209–218

Sklenar V, Piotto M, Leppik R, Saudek V (1993) Gradient-tailored water suppression for h-1-n-15 hsqc experiments optimized to retain full sensitivity. J Magn Reson A 102:241–245

Subbalakshmi C, Krishnakumari V, Nagaraj R, Sitaram N (1996) Requirements for antibacterial and hemolytic activities in the bovine neutrophil derived 13-residue peptide indolicidin. FEBS Lett 395:48–52

Tinoco LW, DaSilva A, Leite A, Valente AP, Almeida FCL (2002) NMR structure of PW2 bound to SDS micelles—A tryptophan-rich anticoccidial peptide selected from phage display libraries. J Biol Chem 277:36351–36356

Vial HJ, Eldin P, Tielens AGM, van Hellemond JJ (2003) Phospholipids in parasitic protozoa. Mol Biochem Parasitol 126:143–154

Whitehead TL, Jones LM, Hicks RP (2001) Effects of the incorporation of CHAPS into SDS micelles on neuropeptide-micelle binding: separation of the role of electrostatic interactions from hydrophobic interactions. Biopolymers 58:593–605

Whitehead TL, Jones LM, Hicks RP (2004) PFG-NMR investigations of the binding of cationic neuropeptides to anionic and zwitterionic micelles. J Biomol Struct Dyn 21:567–576

Wu M, Maier E, Benz R, Hancock REW (1999) Mechanism of interaction of different classes of cationic antimicrobial peptides with planar bilayers and with the cytoplasmic membrane of *Escherichia coli*. Biochemistry 38:7235–7242

Wüthrich K (1986) NMR of proteins and nucleic acids. Wiley-Interscience, New York

Yeaman MR, Yount NY (2003) Mechanisms of antimicrobial peptide action and resistance. Pharmacol Rev 55:27–55

Yu K, Kang S, Kim SD, Ryu PD, Kim Y (2001) Interactions between mastoparan B and the membrane studied by H-1 NMR spectroscopy. J Biomol Struct Dyn 18:595–606

Zasloff M (1992) Antibiotic peptides as mediators of innate immunity. Curr Opin Immunol 4:3–7